Geophysical transect across a Paleoproterozoic continent–continent collision zone: The Trans-Hudson Orogen[1, 2, 3]

D.J. White, M.D. Thomas, A.G. Jones, J. Hope, B. Németh, and Z. Hajnal

Abstract: A summary and comparison of geophysical data and models for the Trans-Hudson Orogen in northern Manitoba and Saskatchewan are presented. Magnetic total field and Bouguer gravity maps are used to define the along-strike extension of geological domains of the orogen exposed on the Canadian Shield, and a two-dimensional density model is produced, which accounts for the observed variations of the Bouguer gravity field across the orogen. An 800-km-long crustal section across the entire continent–continent collision zone, including the edges of the bounding cratonic blocks, is presented. It incorporates seismic reflectivity, seismic velocities, resistivity, and density models. Key results include (1) evidence for west-vergent crustal stacking and exhumation in the eastern Trans-Hudson Orogen in the form of preserved Moho topography and the presence of higher grade (higher velocity) rocks in the hanging wall of an east-dipping crustal stack; (2) definition of the eastward extent of the Archean Sask craton in the subsurface based on distinct lower crustal properties; and (3) 400 m of present-day surface topography and 6–8 km of relief on the Moho are isostatically compensated mainly within the upper mantle by a westward increase in upper mantle temperatures by 40–155 °C and (or) 16–107 km of thinning of the mantle lithosphere.

Résumé : Cet article présente un résumé et une comparaison des données géophysiques et des modèles de l'orogène trans-hudsonien au Manitoba et en Saskatchewan. Les cartes de champ magnétique total et les cartes gravimétriques de Bouguer sont utilisées pour définir l'extension selon la direction des domaines géologiques de l'orogène affleurant dans le Bouclier canadien; un modèle de densité à 2D est produit qui tient compte des variations du champ gravimétrique Bouguer à travers l'orogène. Une section de la croûte de 800 km de long à travers toute la zone de collision continent à continent, incluant les limites des blocs cratoniques à la bordure, est présentée; cette section incorpore la réflectivité sismique, les vitesses sismiques ainsi que des modèles de résistivité et de densité. Les principaux résultats comprennent : (1) des évidences pour un empilement crustal à vergence ouest et de l'exhumation dans la portion est de l'orogène trans-hudsonien, sous la forme de topographie préservée du Moho et la présence de roches plus compétentes (plus grande vitesse) dans l'éponte supérieure d'un empilement crustal à pendage est; (2) la définition de l'étendue, sous la surface, vers l'est, du craton archéen Sask en se basant sur les propriétés distinctes de la croûte inférieure; (3) 400 m de topographie de surface actuelle et 6–8 km de relief sur le Moho sont compensés isostatiquement, surtout dans le manteau supérieur, par un accroissement vers l'ouest des températures du manteau supérieur de 40 à 155 ºC et/ou d'un amincissement de 16 à 107 km de la lithosphère du manteau.

[Traduit par la Rédaction]

Introduction

The crustal architecture of the Trans-Hudson Orogen (THO) in Manitoba and Saskatchewan has been the focus of extensive geoscientific investigation during the past 15 years. Geophysical surveys conducted under the auspices of the Lithoprobe THO transect have been of critical importance in redefining the architecture of the orogen. In this study, we provide a representative summary and comparison of the primary geophysical data in two parts. First, an interpretation of existing potential field maps (magnetic total field and gravity) is presented that identifies the along-strike distribution of the constituent geological domains within the orogen. Secondly, two dimensional (2-D) modelling of the Bouguer

Received 12 November 2003. Accepted 22 November 2004. Published on the NRC Research Press Web site at http://cjes.nrc.ca on 16 June 2005.

Paper handled by Associate Editor R.M. Clowes.

D.J. White,[4] M.D. Thomas, A.G. Jones,[5] and J. Hope. Geological Survey of Canada, 615 Booth Street, Ottawa, ON K1A 0E9, Canada.
B. Németh and Z. Hajnal. Department. of Geological Sciences, University of Saskatoon, Saskatoon, SK S7N 0W0, Canada.

[1]This article is one of a selection of papers published in this Special Issue on *The Trans-Hudson Orogen Transect of Lithoprobe*.
[2]Lithoprobe Publication 1392.
[3]Geological Survey of Canada Contribution 2003215.
[4]Corresponding author (don.white@nrcan.gc.ca).
[5]Present address: Dublin Institute for Advanced Studies, 5 Merrion Sq., Dublin 2, Ireland.

 doi: 10.1139/E05-002

Fig. 1. Simplified geological map of the Trans-Hudson Orogen in Manitoba and Saskatchewan. Shown are the locations of the seismic refraction lines, seismic reflection lines, MT stations and the projection line used for constructing the crustal cross-sections. The seismic refraction lines are R1, R2, and R3; the 1991 seismic reflection lines are 1a–1b, 2–5, 7a–7c, 9, and 10; the 1994 seismic reflection lines are S1a, S2a–S2d, and S3a–S3b. NFSZ, Needle Falls shear zone; BRSB, Birch Rapids straight belt; GCT, Guncoat thrust; SF, Stanley fault; HSZ, Hartley shear zone; TFZ, Tabbernor fault zone; SWF, Sturgeon–Weir fault; ALSZ, Athapapuskow Lake shear zone; SBF, Superior boundary fault.

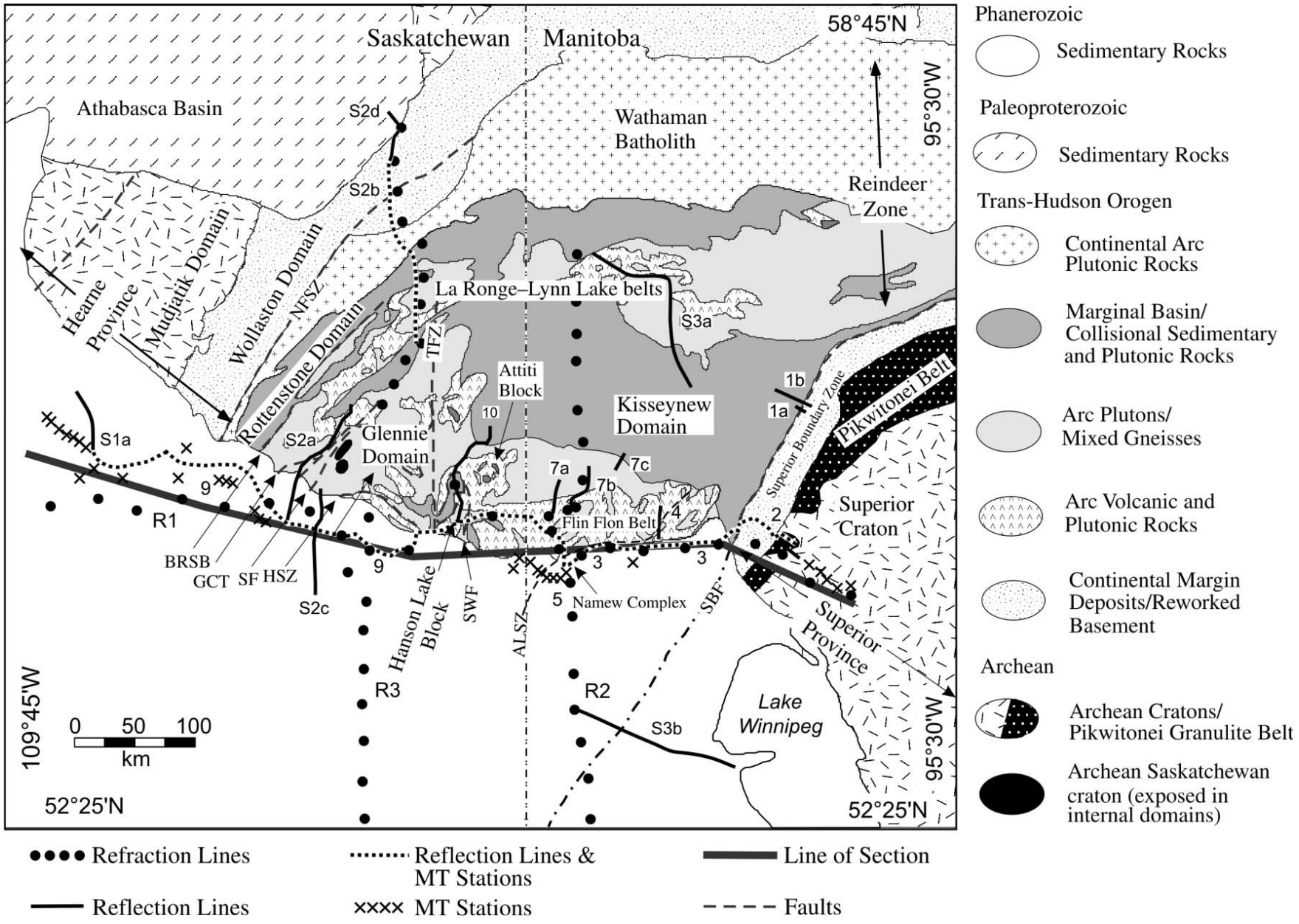

gravity field and the resultant density model for the crust and upper mantle are presented. Finally, the results of the geophysical surveys and their subsequent analyses are used as the basis for constructing an 800-km long crustal section across the entire continent–continent collision zone, including the edges of the bounding cratonic blocks. There are few other orogens in the world where a geophysical transect of this magnitude can be constructed.

The crustal section compares results from the near-vertical-incidence seismic reflection, seismic refraction – wide-angle reflection, magnetotelluric (MT) sounding, and gravity data analyses. All of the data sets and (or) resulting models are projected onto a common line of section (see Fig. 1) to facilitate comparison. Seismic reflection data from the 1991 survey (Lucas et al. 1993; Lewry et al. 1994; Hajnal et al. 1996; White et al. 1999) and the 1994 survey (Hajnal et al. 2005) have been projected onto the line and depth-migrated using velocity models from published analyses of the refraction – wide-angle reflection data (Németh 1999; Németh et al. 2005; Hajnal et al. 2005). The MT data (e.g., Jones et al. 1993, 2005; White et al. 1999; Ferguson et al. 1999) have been inverted to obtain regional-scale resistivity models along the projection line. Density models have been constructed, based on modeling of the Bouguer gravity field, that incorporate the geometry from the seismic interpretations, lower crustal and upper mantle densities calculated from the seismic velocity models, and surface density measurements. Comparison of the data along a planar section removes many of the complications introduced by interpretations of data acquired along crooked lines.

Interpreted magnetic and gravity maps of the Trans-Hudson Orogen

The Trans-Hudson Orogen (Fig. 1) is exposed over a relatively limited strike-length of ~500 km, disappearing under Phanerozoic sedimentary cover to the south and to the northeast. However, gravity and magnetic data indicate that the orogen is much more extensive, following an ~2800-km-long path from South Dakota, USA., to northern Hudson Bay, Canada (Hoffman 1988; Thomas 2001), and possibly continuing as far as Greenland. The following descriptions of the gravity and magnetic fields are made in the context of the established Precambrian geological framework for the exposed Canadian Shield (e.g., Corkery 1987; Macdonald and Broughton 1980) and interpreted Precambrian basement domains modified from Miles et al. (1997) and Pilkington and Thomas (2001). A detailed geological description of the orogen is provided by Ansdell (2005). Discussions of magnetic and gravity data presented here focus on the Precambrian basement south of the shield margin. In the discussions, "extension" is used to identify the buried equivalent of a "domain" or "belt" defined on the exposed Canadian Shield.

Magnetic field map

The basement Precambrian domains were defined principally on the basis of patterns of the total magnetic field and its vertical gradient. Gravity data were used in a supplementary role.

Eastern Trans-Hudson Orogen

The magnetic signature (Fig. 2) of the eastern margin of the THO (the Superior boundary zone (SBZ)) can be traced from the Canadian Shield to the 49th parallel. On the Shield, the west to west-southwest magnetic trends of the Superior Province terminate abruptly against the north-northeast trends of the SBZ. The Pikwitonei gneiss belt is characterized by strong magnetic highs, whereas the eastern half of the SBZ coincides with a magnetic low. The contrast in magnetic patterns has been attributed locally to Hudsonian metamorphic overprinting of granulites in the SBZ, which destroyed magnetite through biotite-, hornblende- or garnet-forming reactions (Bleeker 1990).

This magnetic expression of the metamorphic front can be followed for about 350 km south-southwest from the Canadian Shield margin, over which distance it is accompanied by a series of pronounced, narrow, linear magnetic highs lying close to the interpreted boundary of the Superior Province (because they are so narrow, they are largely obliterated by the line defining the eastern margin of the SBZ in Fig. 2). Based on the exposed SBZ, it is speculated that the magnetic highs are related to metabasalt, metapicrite or banded iron formation found within the Ospwagan Group (Bleeker 1990). Farther south, the eastern boundary of the THO is interpreted to assume a more southerly trend, its position again being assigned principally on the basis of truncation of east–west Superior Province magnetic trends. The position is supported by patterns of linear gravity features.

Southwest from the shield margin, the western boundary of the SBZ is defined by the contrast between the generally low magnetic signature of the SBZ itself and an adjacent irregular pattern of magnetic highs and lows to the west that is attributed to the Flin Flon belt. The broad magnetic low of the SBZ gives way further south to a series of strong positive magnetic anomalies, a magnetic pattern that remains texturally distinct from that of the Flin Flon belt, its extension, and the extensions of the associated (Lucas et al. 1999) Attitti domain and Hanson Lake block, forming a wide north–south belt that narrows southward. The magnetic pattern reflects the mosaic-like nature of felsic, intermediate, mafic and ultramafic intrusions, mafic volcanics and clastic sedimentary rocks, and metamorphic equivalents that characterize the Flin Flon belt on the Canadian Shield. Geophysical mapping of the basement between the shield and latitude 54°N, constrained by basement drill-core samples, provides strong evidence for a southward extension of the belt (Leclair et al. 1997).

Western Trans-Hudson Orogen

The southward extension of the Tabbernor fault zone (TFZ) is interpreted as a southward-widening zone of subdued magnetic relief flanking the Flin Flon belt extension. The interpreted zone is ~15 km wide at the Canadian Shield margin and widens gradually southward to a maximum width of 85 km. Based on the sub-Phanerozoic mapping by Leclair et al. (1997), the subdued magnetic signature of the TFZ is attributed primarily to metamorphic rocks derived from volcanic, volcaniclastic, and plutonic rocks of various compositions, and mafic, calcic, and psammitic gneisses.

Between the TFZ and a parallel belt of low magnetic intensity designated as the Saskatoon domain is the ~190 km

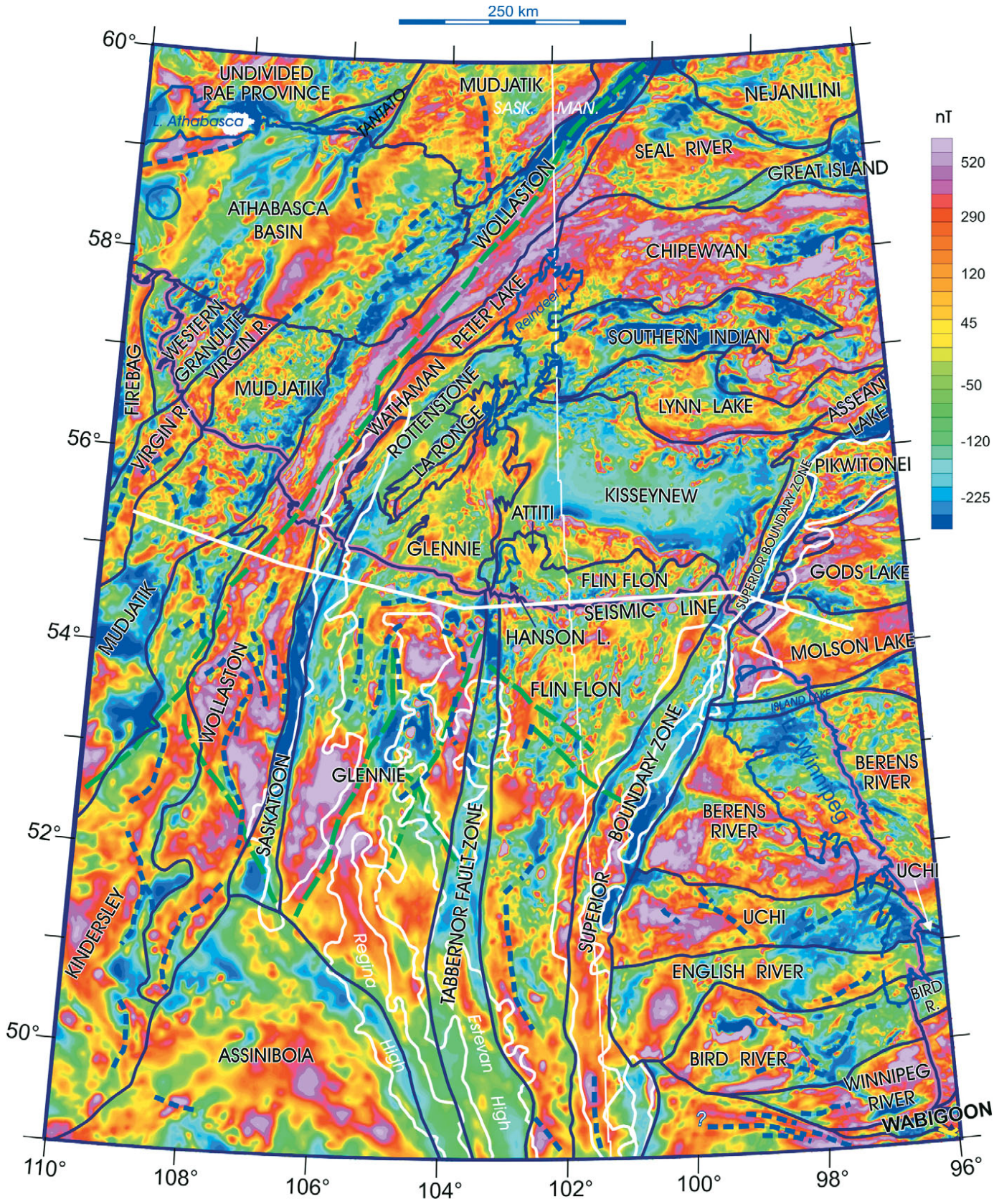

Fig. 2. Total field magnetic map of portions of Saskatchewan and Manitoba with overlay showing principal tectonic domains on the Canadian Shield and their interpreted distribution under Phanerozoic sedimentary cover. The magnetic (and gravity data, Fig. 3) used in this study are obtained from databases maintained by the National Geophysical Data Centre at the Geological Survey of Canada, Ottawa, Ontario. Most aeromagnetic surveys in the region were flown at 805 m line-spacing and 305 m mean terrain clearance (mtc), although mtc and line-spacing range from 119 m and 402 m to 984 m and 3250 m, respectively. All surveys have been levelled to a constant mtc of 305 m. The magnetic total field map is based on a 1-km grid of values. The projection line used for constructing the crustal cross-sections is indicated in white. The other more curved solid white lines are selected zero-value contours from a gravity vertical gradient map (not shown). The short-dash and long-dash lines are specific linear features identified on magnetic and gravity vertical gradient maps (not shown), respectively, that probably delineate faults.

wide interpreted sub-Phanerozoic extension of the Glennie domain. On the exposed shield, the Glennie domain comprises mainly quartz dioritic to granodioritic orthogneisses and plutons, with an associated chaotic magnetic pattern that is comparable to that of the low-grade, plutonic–volcanic Flin Flon belt. This is not surprising considering the proposed continuity between the Glennie domain and Flin Flon belt (Ashton et al. 1999). However, extensive areas of strong, broad positive magnetic anomalies characterize much of the interpreted extension of the Glennie domain, in contrast to the magnetic signature of the Flin Flon belt extension. These north- to north-northwest-trending anomalies are partly coincident with prominent positive gravity anomalies (white outlines in Fig. 2, or see Fig. 3), which may signify the presence of intermediate-mafic granulites (Miles et al. 1997) or mafic volcanic rocks. If this is the case, the Glennie domain extension likely includes a deeper crustal level than exposed on the Canadian Shield.

The Saskatoon domain separates the Glennie domain from the proposed extension of the Wollaston domain to the west, and lies along strike from the Rottenstone domain and Wathaman batholith. The Saskatoon domain is generally 15–35 km wide, widening to ~60 km near its southern termination. It is defined by an apparently featureless prominent magnetic low, though internal texture in the form of discontinuous linear highs is revealed on a vertical gradient map. The western boundary of the domain coincides with the proposed extension of the Needle Falls shear zone (NFSZ). The subdued magnetic field over the domain may, in part, be the expression of a low that is complementary to the adjacent strong magnetic high to the west. Shear zones similar to those within the Birch Rapids straight belt (Coté 1994) along the eastern margin of the Rottenstone domain may also influence the lower level.

The Wollaston domain, dominated by high-grade metamorphosed passive margin sediments, is characterized by strong, linear magnetic highs, the extension of which can be traced several hundred kilometres to the south-southwest. However, the bordering Wathaman batholith is also characterized by a magnetic high, and it is possible that the eastern margin of the Wollaston extension is underlain by a continuation of the Wathaman batholith (e.g., Kreis et al. 2000). If the Wathaman batholith does underlies this region, it implies that the NFSZ cuts across the batholith.

The Mudjatik domain comprises reworked granulitic and migmatitic Archean basement, and produces an irregular magnetic pattern of juxtaposed highs and lows with generally low aspect ratios. This pattern continues southwest under the Phanerozoic cover just beyond the geophysical transect where it is replaced by magnetic lows. South of the transect, the Mudjatik and Wollaston domains are separated by the Kindersley domain, which has no apparent counterpart on the Canadian Shield. The magnetic pattern of the Kindersley domain is similar to that of the Mudjatik domain, but it is distinguished on the basis of differences in trends of anomalies, and the presence of lows within the Mudjatik domain. In the southwest corner of Saskatchewan, the triangular Assiniboia domain (cf., Kreis et al. 2000) is defined based on differences in trends and textures observed on a map of magnetic vertical gradient. It contains prominent magnetic highs having various trends and generally is characterized by a low gravity field.

Gravity field map

The Bouguer gravity field of the THO (Fig. 3) is characterized, generally, by an agglomeration of relatively positive anomalies that are collectively stronger and more positive than those over the flanking Rae, Hearne, and Wyoming provinces to the west. To the east, the Superior Province produces a gravity signature of similar intensity to the THO, but with different anomaly patterns. The stronger anomalies and higher gravity field (generally > –55 mGal (1 Gal = 1 cm s^{-2})) over the Superior Province and THO, contrast with the more subdued response (generally < –55 mGal) over the Rae and Hearne provinces.

Superposed on the Bouguer anomaly map (Fig. 3) is a selection of zero-value contours defining specific gravity highs on a map of the vertical gradient of the Bouguer anomaly. Theoretically, the zero contour of a vertical gradient map coincides with geological contacts (= density domain boundaries) under the assumption that the boundaries are steep.

Eastern Trans-Hudson Orogen

Two prominent subparallel series of linear to curvilinear gravity highs trending south-southwest from the Canadian Shield margin correlate with the sub-Phanerozoic extension of the SBZ, as defined by magnetic interpretation. The broader western series is essentially continuous and extends to latitude 49°N, whereas the eastern series is narrower, discontinuous, and absent between 51°N and 50°N. The western series is associated with positive magnetic anomalies, particularly along its southern portion (Fig. 2). This combination of strong positive gravity and magnetic anomalies may signify the presence of granulite-grade, Pikwitonei-type gneisses (Miles et al. 1997), although the belt of gravity anomalies is offset westward from a similar belt over the exposed Pikwitonei gneisses (Fig. 3). The eastern series of gravity highs coincides with a neutral or negative magnetic signature. Modelling of the two belts of gravity highs west of Lake Winnipeg along line S3b (Surasky et al. 2001; see Fig. 1 for location) attrib-

Fig. 3. Bouguer gravity anomaly map corresponding to area of Fig. 2 based on a 4-km grid of values with overlay showing mapped and interpreted tectonic domains. Gravity observations are generally spaced 10–15 km apart with finer spacing in some regions. The projection line used for constructing the crustal cross-sections is indicated in blue. The solid white lines are selected zero-value contours from a gravity vertical gradient map (not shown). The short-dash and long-dash lines are specific linear features identified on magnetic and gravity vertical gradient maps (not shown) that probably delineate faults.

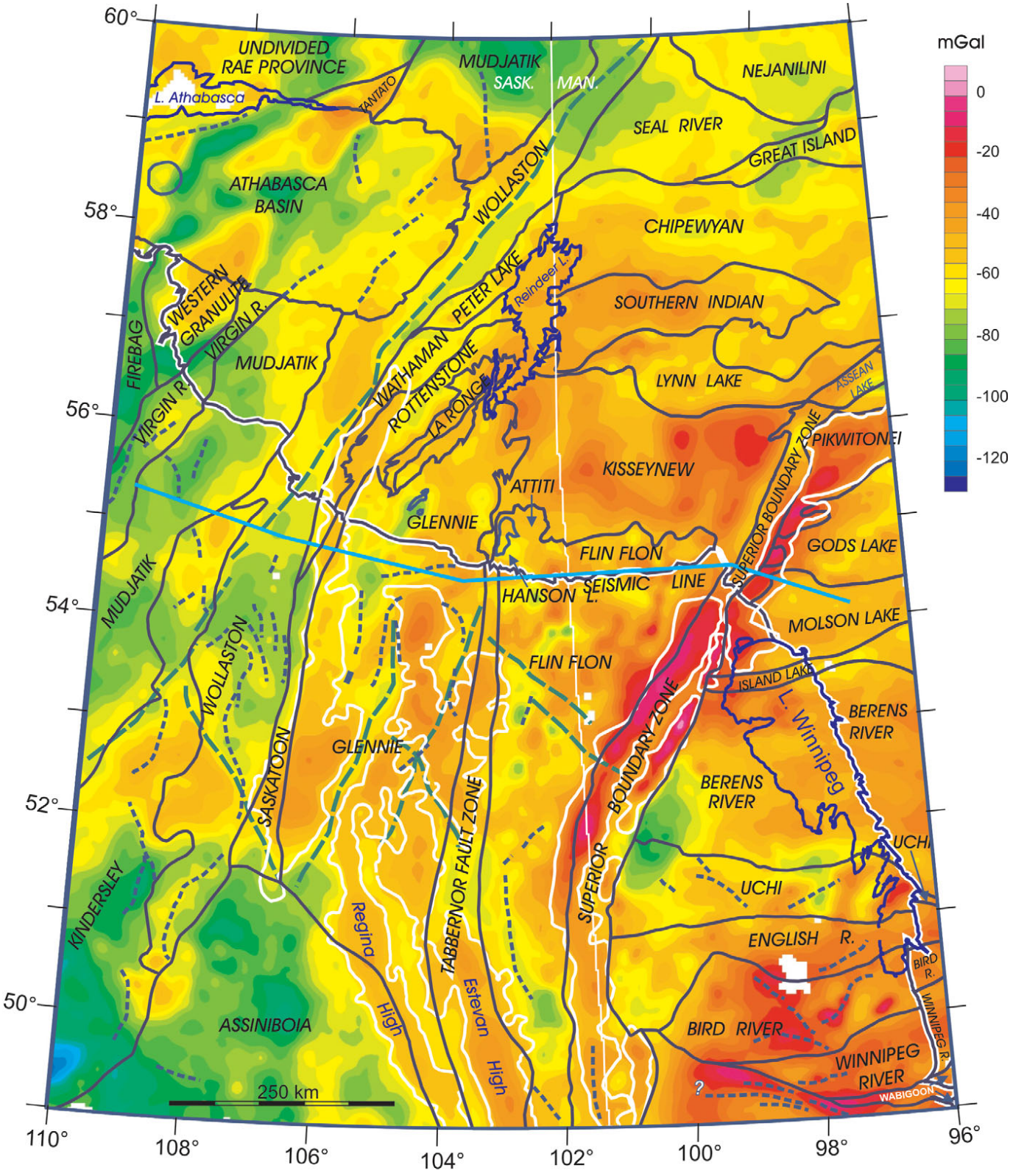

Fig. 4. (*a*) Bouguer anomaly along the geophysical transect extracted from the gravity field shown in Fig. 3, and elevation along the transect determined from the elevation map shown in Fig. 5. A polynomial regression curve (3 degrees) fitting the Bouguer anomaly profile exhibits a westward increase of about 10 mGal over the first 200 km and then decreases by about 35 mGal across the remaining 620 km. Elevation increases by ~400 m from east to west across the profile. (*b*) Plot of elevation versus Bouguer anomaly for area of Saskatchewan and Manitoba shown in Fig. 5, and a linear regression line. A linear regression line determined by Simpson et al. (1986) for a plot of elevation versus Bouguer anomaly for the conterminous United States is shown for comparison.

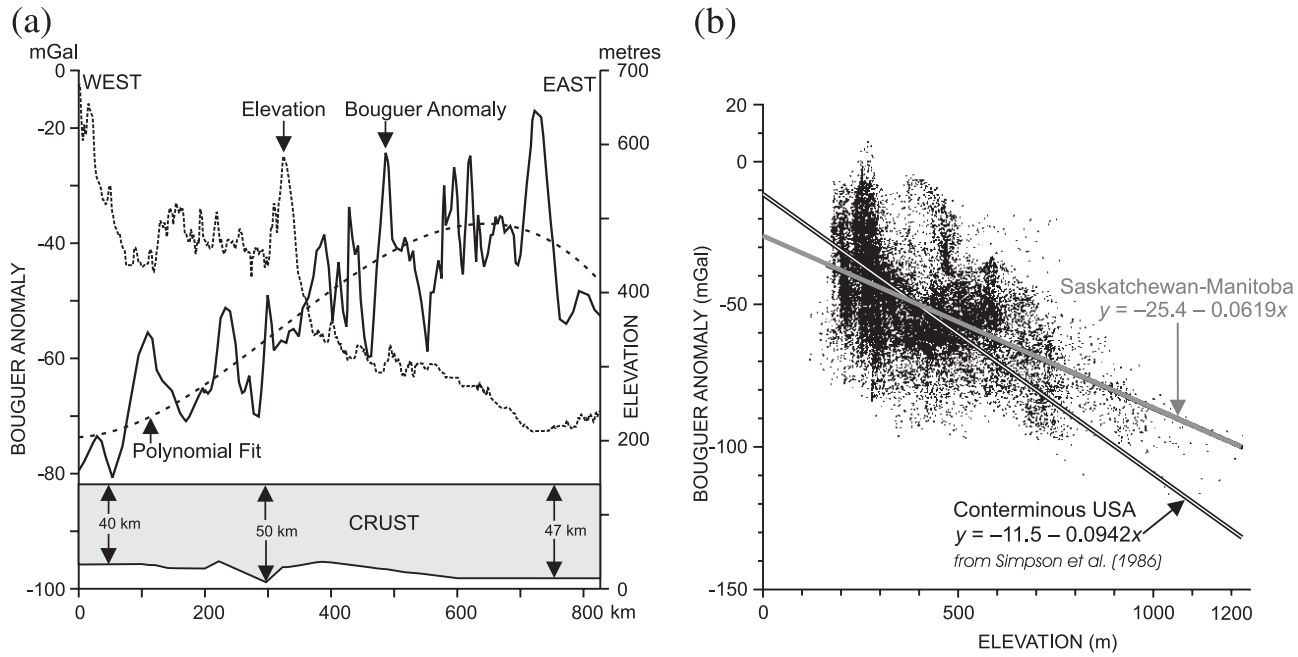

utes the western belt to metasedimentary rocks typical of the Kisseynew domain and the eastern belt to metasedimentary rocks of similar affinity or with correlative supracrustal rocks of the Superior boundary zone (White et al. 2002) and an underlying layer of tholeiite.

Over the Flin Flon belt and its sub-Phanerozoic extension, the gravity field is characterized by a mosaic of highs and lows of generally limited extent, many with an oval shape. This pattern is typical of what might be expected over this interpreted granite–greenstone domain.

Western Trans-Hudson Orogen

The western THO is characterized by a series of strong linear gravity highs trending from NNW to NNE in close juxtaposition. At the southern end of the TFZ, the correlation of the Estevan gravity high with a subdued magnetic field has been attributed to the presence of Kisseynew-type gneisses (Miles et al. 1997). In the northern part of the TFZ, a positive gravity anomaly extends into the eastern part of the Glennie domain extension, suggesting that the source of the anomaly may be deeper than that of the magnetic signature defining the boundary between these two domains. Alternatively, the source of the gravity anomaly may be westward dipping. The same argument may be applied to the migration of a gravity high across the western boundary of the Glennie domain extension into the Saskatoon domain. Most of the Glennie extension is characterized by broad, extensive gravity highs. One noteworthy low occurs near the geophysical transect on strike with another low that embraces the Archean Hunter Bay and Istwatikan inliers on the Canadian Shield. At the south end of the Glennie extension, an extensive linear gravity high (Regina high) straddles the boundary with the Assiniboia domain.

The generally positive gravity expression of the Wathaman batholith contradicts the normal association of granitic batholiths and negative gravity anomalies. Negative anomalies are observed over parts of the Chipewyan batholith (Fig. 3), but these are not pronounced. A linear gravity high straddling the boundary between the Wathaman batholith and Rottenstone domain on the Canadian Shield migrates progressively into the western margin of the Glennie extension, continuing and broadening towards the south, where it also embraces part of the Saskatoon domain. These transgressions are consistent with sources at greater depth than those related to magnetic signatures defining the domain boundaries or with west-dipping domains. Most of the Wollaston and Mudjatik extensions correlate with broad, extensive negative gravity signatures, whereas the signature of the intervening Kindersley domain is variable.

Long-wavelength trend

The Bouguer gravity field in Manitoba and Saskatchewan is characterized by a regional westward decrease (Fig. 4*a*) accompanied by a corresponding increase in elevation (Figs. 4, 5). The inverse relationship between Bouguer anomaly and elevation observed here (Fig. 4*b*) is an example of a more general relation that has long been recognized and is commonly attributed to compensation of topographic loads by complementary crustal roots (i.e., Airy isostasy). The roots represent a negative density contrast with respect to laterally adjacent mantle and produce negative Bouguer gravity anomalies. The mechanism of compensation for the region is ex-

Fig. 5. Elevation (metres) map for the same area of Manitoba and Saskatchewan shown in Figs. 2 and 3. Line of geophysical transect used for constructing the crustal cross-sections is indicated.

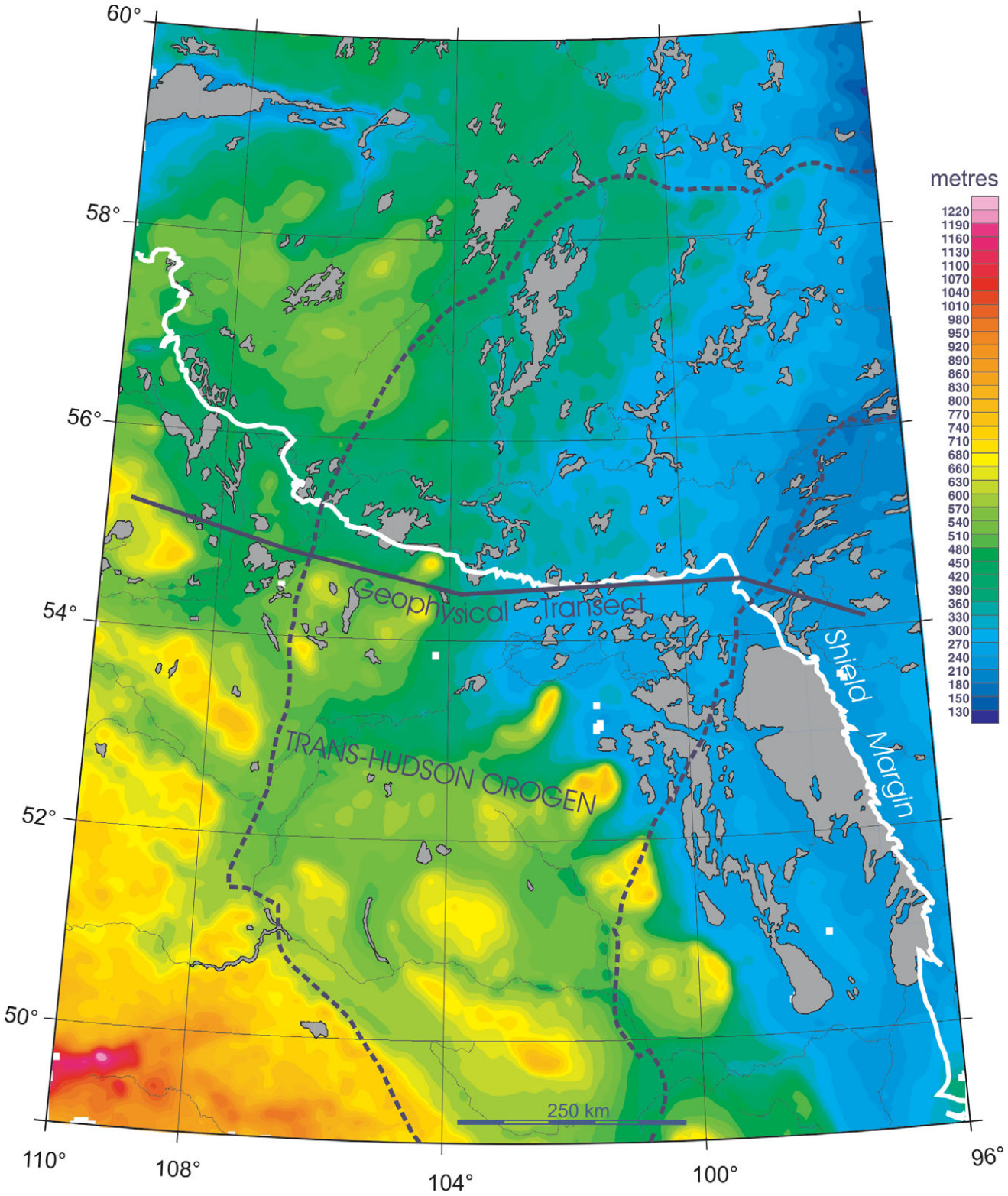

Fig. 6. Two-dimensional gravity model along the geophysical transect. Density units in the lower part of the section, below 19 km depth, are based on the seismic refraction velocity model of Németh (1999) (see Fig. 7*d*). ALSZ, Athapapuskow Lake shear zone; FFB, Flin Flon belt; HB, Hansen Lake block; KGB, Kisseynew gneiss belt; LRB, La Ronge belt; NFSZ, Needle Falls shear zone; NGC, Namew gneiss complex; PG, Pikwitonei gneiss; RD, Rottenstone domain; SBF, Superior boundary fault; SBZ, Superior boundary zone; SF, Stanley fault; SWF, Sturgeon–Weir fault; TFZ, Tabbernor fault zone; VR, Virgin River; WB, Wathaman batholith; WG, Western Granulite.

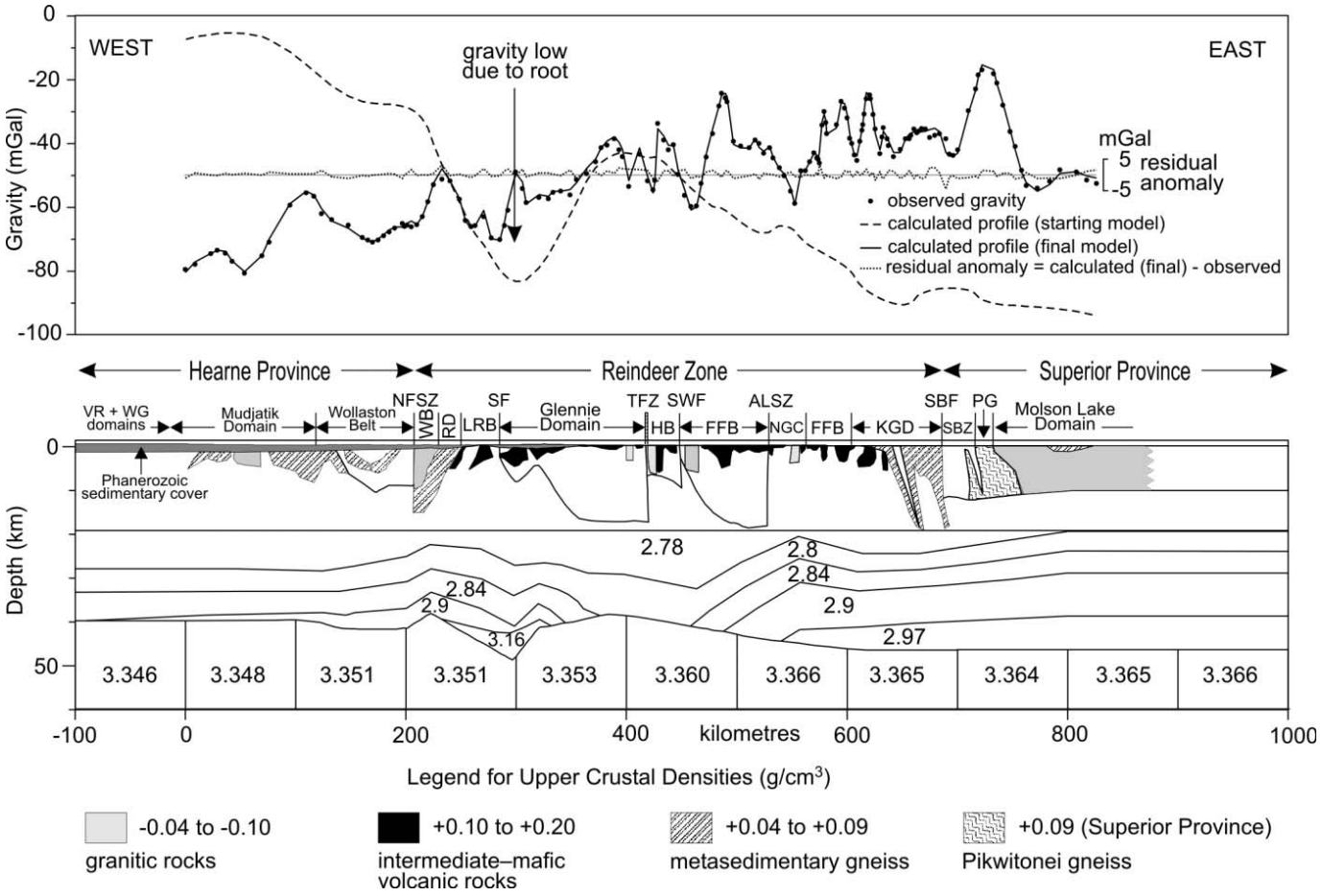

amined in more detail in the following discussion of gravity modeling.

Gravity modelling and the density model

Construction of an initial density model

A seismic refraction – wide-angle reflection velocity model from Németh (1999) (reproduced in Fig. 7*d*) was used to derive a corresponding 2-D initial density model as a constraint for gravity modelling. Velocities were converted to corresponding density values using well-known empirical relationships. The Nafe-Drake relationship (Ludwig et al. 1970) was used for upper and lower crustal rocks with velocities ≤6.8 km/s, a granulite metamorphic grade relationship (Christensen and Fountain 1975) was used for lower crustal rocks with velocities ≥6.8 km/s, and a formula for ultrabasic mantle rocks (Christensen 1966) was used for the upper mantle. It is recognized that uncertainties of up to ±5%–8% (Barton 1986) can be involved in the conversion from velocity to density for crustal rocks in the absence of any other constraints. Also, 2-D gravity modelling is inaccurate in cases where the strike length of the density constrast is not many times greater than its depth, and thus, although the density profile is generally oriented normal to strike, there will be significant uncertainty in the results because of unknown finite strike-length effects. However, many of the interpreted crustal-scale domains (see Figs. 2, 3) appear to have strike-lengths on the order of hundreds of kilometres, providing some assurance that 2-D gravity modelling is not without validity.

The density model (Figs. 6–8) consists of a surface veneer of Phanerozoic sedimentary rocks overlying a crustal section that thickens from 40 km in the west to 45–48 km in the east. The crust is divided into an upper layer ranging in thickness from 12 to 21 km and a lower layer ranging from 20 to 30 km thick. Calculated densities of the upper crust range from 2.73 to 2.78 g/cm^3, and of the lower crust from 2.78 to 2.98 g/cm^3. Mantle within the model extends to 100 km in depth and ranges in density from 3.34 g/cm^3 to 3.37 g/cm^3. Lithosphere below this depth is assigned a uniform density of 3.37 g/cm^3. Density variations within the upper crust and mantle are small, being ~1.8% and 0.8%, respectively, whereas larger density variations (7%) are observed within the lower crust.

Table 1. Summary of rock density information.

Rock unit and (or) rock-type(s)	Location	Mean density (g/cm^3)
Trans-Hudson Orogen		
Burntwood Suite	Kisseynew gneiss belt	
• Metasedimentary gneisses	• Lithoprobe line 1b	2.83
	• Lithoprobe line 7a	2.76
	• Lithoprobe line 7c	2.79
Burntwood Suite	Kisseynew gneiss belt	
• Metasedimentary gneisses		2.72*
Missi Suite	Margin of Kisseynew gneiss belt	
• Metasedimentary gneisses	• Lithoprobe line 7a	2.77
	• Lithoprobe line 7c	2.81
	• In and near Flin Flon	2.71
	Flin Flon belt	
• Juvenile arc basalts, basalts-andesites (inc. volcanoclastics)	• Near Flin Flon	2.83
• Ocean-floor mafic volcanics	• Near Flin Flon	3.02
• Juvenile arc mafic volcanics	• Reed Lake	2.81
• Rhyolites	Flin Flon belt	2.65
• Granites	Flin Flon belt	
	• Reed Lake granite	2.70
	• Various small granite bodies	2.64
Superior Province		
• Mixed gneisses	Southern Superior boundary zone	
	• line 2	2.70
• Mixed gneisses	Northern Superior boundary zone	
	• Paint Lake near line 1a	2.77
• Mixed gneisses	Molson Lake/Gods Lake domains	
	• near line 2	2.69
Pikwitonei gneiss	• line 2	2.80
• Mixed gneisses	• Sipiwesk Lake	2.84**

Note: *McGrath (1991); **Thomas and Tanczyk (1994).

The gravity profile calculated for the initial density model is illustrated in Fig. 6 together with the observed Bouguer gravity field along the refraction line. There are significant disparities between the observed and calculated gravity curves: (1) large amplitude (up to ~30 mGal) short wavelength variations in the observed gravity are absent from the calculated curve, (2) a large ~45 mGal low on the calculated profile in the region of local crustal thickening is absent in the observed Bouguer profile, and (3) an ~80 mGal westward increase in calculated gravity related to the westward decrease in crustal thickness, conflicts with a decrease of similar magnitude in the observed profile. If the geometries of crustal layers in the refraction model are realistic, densities derived from the seismic velocities must be unrepresentative for certain elements of the crust and upper mantle in this region.

The first disparity is expected, because short-wavelength components of the gravity profile are associated with shallow density variations generally occurring on a scale that is not resolved by the refraction velocity model. The second discrepancy suggests that the density contrast between the lower crust and upper mantle must be reduced in the vicinity of the crustal root, and the third mismatch requires a westward decrease in density within one or more of the principal layers, to counteract the effect of westward-thinning crust. Each of these elements of the model is considered in the following sections.

Detailed gravity modelling of the upper crust

A relatively detailed gravity model of the upper crust (the top 20 km) is presented in Figs. 6–8. It is constrained by surface geology, density measurements on rock samples from the eastern part of the THO (summarized in Table 1), and geometries of crustal units defined by seismic reflection data. Density contrasts rather than absolute densities are used in the upper crust as the increase of density with depth implied by the velocity information is more easily accommodated in this manner. A near-surface background density of 2.69 g/cm^3 is assumed based on values determined for areas of felsic–intermediate gneisses in the SBZ and for granitoids and gneissic granitoids in the Molson Lake – Gods Lake domains.

Most upper crustal bodies modelled in Figs. 6–8 extend from the Precambrian surface to maximum depths of about 5 km. Notable exceptions are bodies of Pikwitonei gneiss (12 km), Kisseynew gneiss (19 km), the Rottenstone domain (15 km), and Wathaman batholith (9 km). In the Superior Province, the uppermost 10 km of crust is modelled with a density contrast of –0.045 g/cm^3, to reproduce the locally lower background level of the gravity field. This implies an absolute density of 2.645 g/cm^3, suggesting a granitic com-

Fig. 7. Compilation of geophysical cross-sections. (*a*) Depth-migrated seismic reflection data obtained by projection on to the section line and depth-migrated using the velocities from (*d*). Pink dashed lines indicate interpreted crustal domain boundaries or prominent structures. Blue dashed line indicates the refraction Moho from panel (*d*). (*b*) Density model obtained by numerical simulation of observed gravity profile using geometry and density constraints from the seismic velocity model and the seismic reflection interpretation. See Fig. 6 for legend of upper crustal densities. Annotated density values have units of gm/cc. (*c*) Seismic velocity anomalies determined by subtracting average 1-D velocity model from the velocity model shown in panel (*d*). (*d*) Seismic velocity model obtained by inversion of the R1 seismic refraction/wide-angle reflection travel times and amplitudes (from Németh 1999). (*e*) Electrical conductivity model from MT data projected on to the section line and inverted. See Figs. 1 and 6 for explanation of abbreviations. B., batholith.

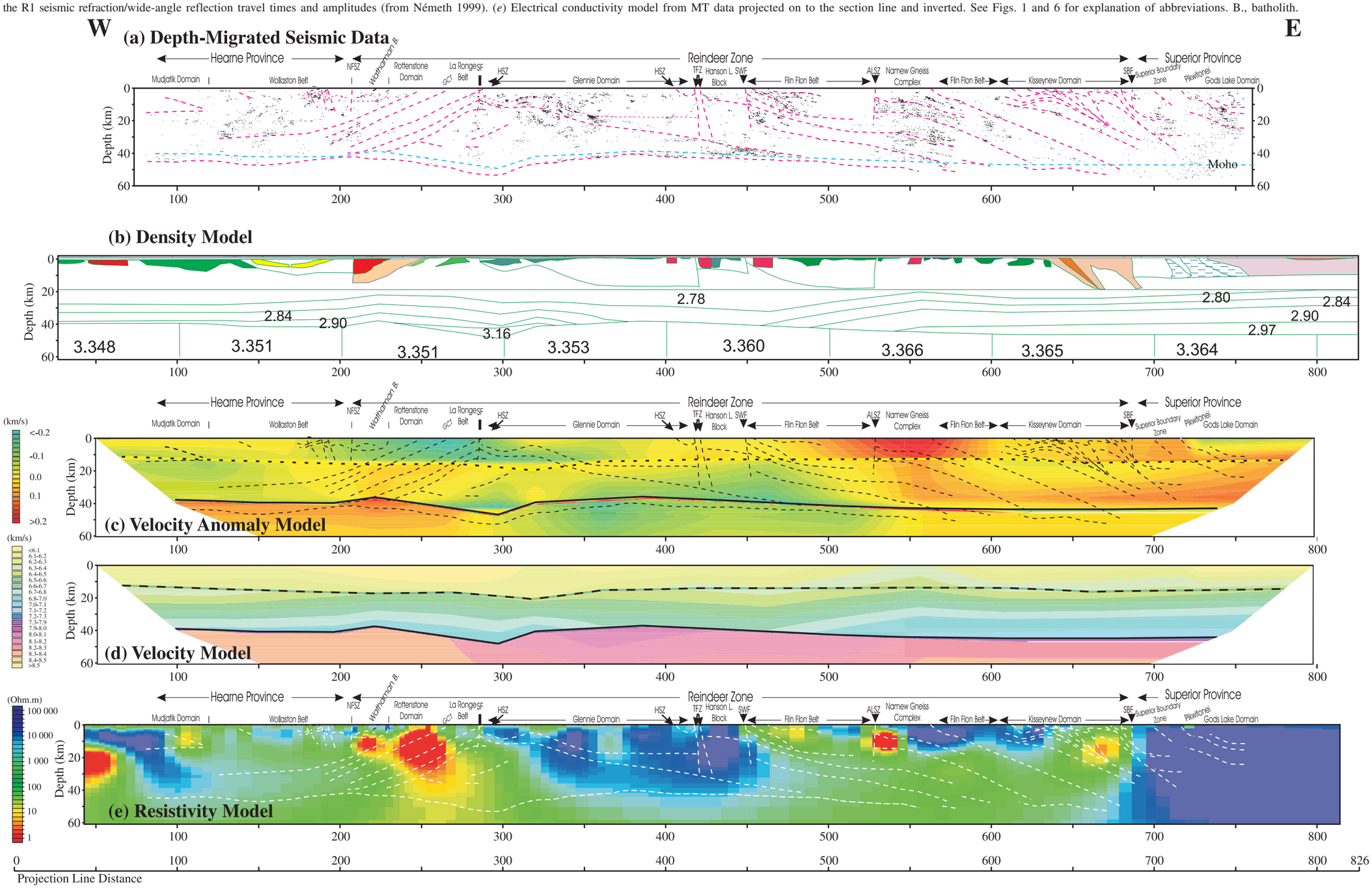

Fig. 8. Cartoon summarizing the crustal architecture across the THO as determined by integrating the geophysical cross-sections shown in Fig. 7. The seismic reflection interpretation is used as a framework for defining subsurface geological domains based on their geophysical (reflectivity, resistivity, velocity, and density) characteristics and relation to the surface geology (either exposed or inferred from potential field interpretation). NACP, North American Central Plains conductivity anomaly). Symbols: ρ_E, electrical resistivity; ρ, density; ΔV indicates the velocity anomaly relative to an average 1-D velocity model; subscripts UC, LC, and M refer to upper crust, lower crust, and mantle, respectively. See Figs. 1 and 6 for explanation of abbreviations. B., batholith.

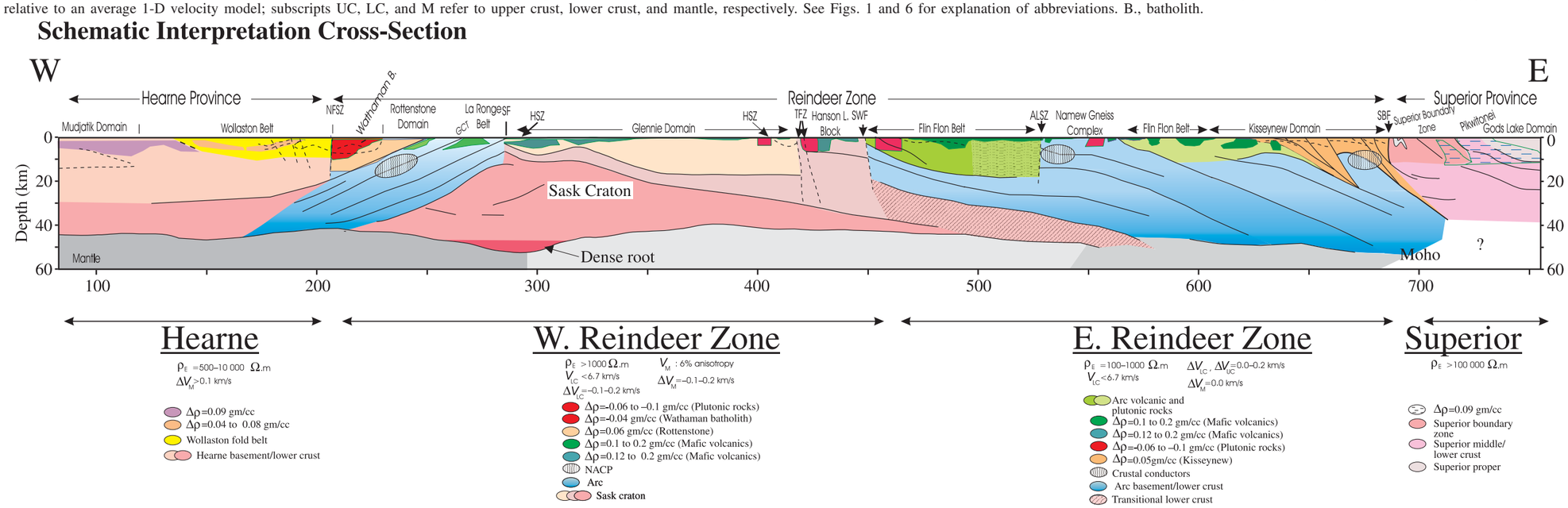

position. Alternatively, the change in level of the field across the Superior boundary zone might be related to upper crust under the Flin Flon belt being more dense than the assumed background density of 2.69 g/cm^3. In the Superior Province a major gravity high extending along the series of exposures of Pikwitonei gneiss (Fig. 3) is attributed to steeply east-dipping blocks of this gneiss that attain a depth of about 11 km. The lateral extent of these gneisses (absolute density of 2.78 g/cm^3) is much greater than indicated in the reflection model. West of the Superior boundary zone, the reflection model portrays the Kisseynew gneisses as a steeply east-dipping package affected by folding and steep faulting, and the gravity model is consistent with this picture. The interpretation of eastward dips for both the Kisseynew and Pikwitonei units differs from the opposing dip model of Surasky et al. (2001) derived for a seismic–gravity transect (line S3b, Fig. 1) located about 165 km southwest of the shield margin. A noteworthy result within the Flin Flon belt is the generally small thickness (~2 km) of juvenile arc volcanics in the east (around the town of Flin Flon) in contrast to a thicker root (~5 km deep) occurring further west.

A significant gravity high over the Rottenstone domain is attributed to an ~15 km-thick slab dipping west beneath the Wathaman batholith to a depth of 15 km. It has a density of 2.75 g/cm^3, consistent with a metasedimentary composition. This westward dip is compatible with dips portrayed in the reflection model and derived by modeling of magnetotelluric data (Jones et al. 1993). The Wathaman batholith is modelled as a triangular body wedged between a vertical Needle Falls shear zone and the inferred metasedimentary slab representing the Rottenstone domain. West of the NFSZ several upper crustal bodies extending from the Precambrian surface to depths ranging from about 2.5 to 8 km are present in the gravity model. Most have positive density contrasts (0.04–0.09 g/cm^3) suggesting a mainly metasedimentary composition.

The crustal root

A zone of crustal thickening centred roughly 300 km from the west end of the transect and observed in both the seismic refraction model and seismic reflection images (Fig. 7) is responsible for a large mismatch between the observed and calculated gravity profiles. Lower crustal and upper mantle densities within the initial density model range from 2.8 to 2.97 g/cm^3 and 3.35 to 3.37 g/cm^3, respectively, resulting in a crust–mantle contrast ranging from 0.40–0.56 g/cm^3. Values in this range are relatively high in comparison to values reported in other studies; cf. 0.35 g/cm^3 in the the conterminous USA (Simpson et al. 1986), 0.31–0.47 g/cm^3 in the Grenville Province (Louden and Fan 1998; Eaton and Hynes 2000), and 0.18–0.30 g/cm^3 to the west of the present study area (Lemieux et al. 2000).

Lowering the density contrast across the Moho would be a simple way to eliminate the mismatch, and could be achieved by locally decreasing mantle densities and (or) increasing lower crustal densities, with appropriate modification of densities in the overlying crust. It is possible, also, that the amplitude of the calculated low may be artificially high, because the 2-D modeling has assumed an infinite strike length for the root; if the latter has a limited strike length it would produce a smaller negative anomaly. We favour increasing the density of the root (from 2.9 g/cm^3 as predicted by the velocity model, to 3.16 g/cm^3 (Fig. 6)), as the root constitutes a local anomaly in crustal thickness and thus might be expected to have anomalous character. Alternatively, a local decrease in upper mantle density was considered less likely, because, peridotites have relatively little variation in density (3.23–3.32 g/cm^3; tables 3–5 of Babuska and Cara 1991), and we assume that eclogites are not present (see "Discussion"). A density increase within the overlying crust cannot be ruled out, but there is no obvious reason as to why this would occur in association with the crustal root. To hide the required density anomaly (associated with a 10 km thick root, with density contrast of 0.53 g/cm^3) in a 20 or 40 km thickness of overlying crust requires a crustal density anomaly of 0.125 g/cm^3 or 0.25 g/cm^3, respectively. If the empirical velocity–density formulae allow for ±5% uncertainties in the resultant densities, then an uncertainty of 0.14 g/cm^3 applies to an estimated density of 2.8 g/cm^3.

Long-wavelength gravity trend

The third discrepancy is the westward increase in gravity predicted by the density model, which contradicts the westward decrease in the observed Bouguer gravity field. The westward decrease in Bouguer gravity by ~35 mGal (to ~–80 mGal) and the complementary increase in elevation by ~400 m over 800 km (Fig. 4) is part of a very broad regional trend (Figs. 3, 5) that continues to the Canadian Cordillera where gravity values reach a minimum of ~–150 mGal. It is clear that if this large negative Bouguer anomaly is due to isostatic compensation, then compensation is achieved primarily within the mantle (e.g., Kane and Godson 1989), with a possible partial contribution from lateral density variations in the crust. It is not achieved by a simple westward increase in crustal thickness. Across the THO the crust thins westward from 45–48 km in the east to ~40 km, with similar crustal thicknesses observed further west across the Western Canada Sedimentary Basin (see Ross et al. 1995) and approaching the Cordillera, where maximum measured crustal thickness is ~50 km (Cook et al. 1992; Zelt and White 1995).

The westward increase in elevation and the corresponding decrease in crustal thickness across the THO, both represent mass excesses that require compensation. Using an average density of 2.67 g/cm^3 for the surface topographic load and a density contrast of 0.4 g/cm^3 across the crust–mantle boundary, the ratio of these relative mass excesses is 1.1:3.2. Thus, the crustal thickness variation is the more significant factor of the two. If these combined effects are compensated for by density variations alone in the upper or lower crust (15 or 25 km thick, respectively), a westward regional decrease in density of 0.28 or 0.17 g/cm^3 would be required in the respective layers. These translate to regional velocity decreases of 1.7 or 0.39 km/s, using Nafe-Drake and granulite facies relations for the upper or lower crust, respectively, which are much greater than the observed westward increase in velocities (Fig. 7*d*). Clearly, compensation within the upper mantle is required. If compensation occurs over the upper 50–200 km of the mantle, expected westward density decreases range from 0.02 to 0.005 g/cm^3, respectively, with associated expected velocity decreases ranging from 0.08 to 0.02 km/s (using the relation from Christensen 1966). A

westward decrease in mantle densities by 0.021 g/cm^3 (from 3.367 g/cm^3 in the east to 3.346 g/cm^3 in the west, and extending to 150 km depth) has been included in the density model (Fig. 6) to match the observed gravity profile. Upper mantle velocities at 50 km depth actually show a westward increase by ~0.1 km/s (Fig. 7*d*). Thus, the inferred mantle density variations must either occur at depths below this, or the small velocity variation may be reflecting compositional or fabric (i.e., anisotropy) variations that have minor effect on density.

Construction of the crustal cross-section

The profile along which the crustal cross-section was constructed is shown in Fig. 1. A profile was chosen that is oriented at a large angle to the regional geological strike while remaining close to the original geophysical profiles. The data or data-based models are projected onto the line of section along normals drawn from the line of section. Similarly, the geological boundaries are projected onto the line of section from where they intersect the seismic reflection profiles. As such, the geological boundaries indicated on the section are close to, but not coincident with either the actual positions of these boundaries, where they intersect the line of section, nor with the projected positions of points, where the geological boundary is intersected by the various geophysical profiles. To ensure valid intercomparison between the geophysical models, the positions of each of the models at major geological boundaries (NFSZ, SF, TFZ, SWF, ALSZ and SBF, see Fig. 1 caption for full names of abbreviations) are aligned. Thus, in this sense, the section is schematic.

The seismic reflection data set

The seismic reflection data presented here (Fig. 7*a*) were acquired in 1991 and 1994. Interpretations of time-migrated data from the first survey (lines 2, 3, 5, and 9) are published (Lucas et al. 1993, 1994; Lewry et al. 1994; White et al. 1994; Hajnal et al. 1996; White et al. 1999), whereas the 1994 data (line S1a) are presented here and in Hajnal et al. (2005) for the first time. Data acquisition parameters and processing (see White et al. 1999) for the two vintages of data were similar and, thus, required minor reprocessing for this compilation. The primary objective of reprocessing the data was to produce accurate depth sections. Toward this end, the data were (1) projected onto the straight line segments of the line of section (Fig. 1), and (2) depth-migrated with a phase-shift frequency-wavenumber (*f-k*) algorithm (Gazdag 1978) using velocity information from the coincident refraction – wide-angle reflection profile (described in the following section) that was not available at the time of the original processing.

Projection of data prior to migration is important for two reasons. First, for data acquired oblique to geological strike, projection onto a strike line results in apparent dips in the section that more closely represent the true geological dips (see White et al. 1999 for a more extensive discussion). This is best done prior to migration, as the migration process is inherently dip-dependent (i.e., the steeper the dips of the unmigrated data, the further they move laterally and up-dip, and the more they steepen during migration). Secondly, data acquired along a crooked line, and presented as a 2-D section will have apparent dip variations that are exclusively the result of the acquisition geometry. The migration process as applied assumes a 2-D planar geometry and thus, the apparent dip variations due to crooked line geometry will introduce artifacts when migrated.

The original time migrations in the previously published work were undertaken using a single velocity (6 km/s) for the entire crust. Use of the refraction velocities is particularly important in achieving the proper reflection geometry at depth, where the refraction velocities are typically much higher (~7 km/s in the lower crust and ~8 km/s in the upper mantle) than the velocity assumed for the original migrations (6 km/s; cf. White et al. 1999). Depth-migrated seismic sections allow the direct comparison of depths in the seismic refraction models with those on the seismic reflection sections. Semblance filtering and amplitude scaling were the only other post-stack processes applied.

The seismic refraction – wide-angle reflection velocity model

The seismic refraction – wide-angle reflection velocity model shown in Fig. 7*d* is from Németh (1999). Details of data acquisition and data analysis can be found in Németh (1999) and Németh et al. (2005). The velocity model depicts the velocity structure of the crust and uppermost mantle in terms of distinct layers that are separated by subhorizontal boundaries (dashed and solid lines) across which the velocities change abruptly. The semi-continuous layer boundaries within the model are required by specific characteristics of the data, such as abrupt changes in apparent velocities and reflections that are observed for most shot points along the profile.

The spatial resolution within the velocity model is limited primarily by the shot spacing (25–50 km) and vertical resolution generally exceeds horizontal resolution. The lateral extent of a velocity inhomogeneity that will be resolved in the velocity model varies with depth: 25–50 km in the upper crust, 50–100 km in the lower crust (with the exception of the Moho where it is 20–40 km), and ~100 km in the upper mantle (e.g., Zelt and White 1995). Typical absolute uncertainties in velocities and layer depths are ±0.1–0.2 km/s in the upper crust, ±0.2 km/s and ±2 km in the lower crust, ±2 km (at the Moho), and ±0.05 km/s within the upper mantle.

The MT resistivity model

MT data acquired within the THO are described in Jones et al. (1993), White et al. (1999), and Ferguson et al. (1999) and are summarized by Jones et al. (2005). The resistivity model presented in Fig. 7*e* is the result of projecting the MT sites onto the projection line followed by data inversion using the RLM2DI inversion algorithm of Rodi and Mackie (2001). This algorithm seeks the smoothest conductivity profile, such that the value of a functional that includes the derivatives of the conductivity with respect to depth and in the horizontal direction along the profile is minimized simultaneously with misfit. An iterative solution is obtained by repeatedly solving for small changes in the conductivity profile at each site, such that the new conductivity produces a smaller residual error between the modelled data and measured data at each

station. Lateral resolution of resistivity anomalies is largely controlled by the station interval, which ranges from 10–20 km. For further details refer to Jones et al. (2005).

Comparison of the geophysical models

The various geophysical models are compared in Fig. 7, and a summary of observations is provided in Fig. 8. In general, there is not a one-to-one correlation between variations observed in the different models, nor of the geophysical variations with the major lithotectonic domains. Recognizing the geological characteristics that each of the geophysical methods are most sensitive to, inferences can be made about the subsurface characteristics of the lithotectonic domains.

As the seismic reflection data provide the most graphic image of the subsurface, we use it as the basis for comparison. Density is controlled by bulk composition in the absence of significant temperature variations, with the bulk density being a representative volume average of the density of the constituent minerals. Similarly, seismic velocities are generally representative of bulk composition for non-porous isotropic rocks. However, values of velocity or density do not uniquely identify composition. Furthermore, for mantle rocks, velocity variations due to anisotropy can be larger than composition-induced changes. In contrast to density and seismic velocity, bulk conductivity is controlled by the presence and interconnectivity of certain conductive minerals (e.g., graphite and sulphides) under fluid-absent conditions. The presence of minor amounts of these minerals can completely dominate the bulk conductivity. Thus, conductivity can be a powerful tool for imaging different crustal domains and structures, but in general, it does not directly constrain the bulk composition in the presence of conducting features.

Inspecting the various geophysical models in Fig. 7, four distinct zones of crustal structure and properties can be identified that generally correspond to the surface lithotectonic domains associated with the Hearne Province, western (Rottenstone, La Ronge, and Glennie domains) and eastern (Flin Flon and Kisseynew domains) Reindeer Zone, and Superior Province. This subdivision is best seen in the seismic reflection and conductivity models, and to a lesser degree in the seismic velocity model. Each of these regions is discussed in turn. Discussion focuses on the relative variation of the different parameters, and thus in the case of velocities or densities, which generally increase with depth, descriptive terms like *low*, *intermediate*, or *high* are relative to other values of these parameters at similar depths.

Hearne margin

The Hearne margin, including the Wollaston and Mudjatik domains, is characterized generally by intermediate-to-high resistivity (5.0×10^2–10^4 Ω.m) and slightly reduced (–0.05 to –0.1 km/s) lower crustal seismic velocities. Further west, there is a zone of low resistivity (10 Ω.m or less) within the lower crust beneath the Hearne craton proper. The upper crust (0–10 km depth) of the eastern Wollaston domain is distinguished by undulating reflections, high resistivity (mainly $>10^3$ Ω.m), intermediate velocities, and low densities. The Wollaston domain contains a significant component of infolded high metamorphic grade metasediments, whereas the Mudjatik domain to the west, characterized by less upper crustal reflectivity and higher densities extending to >5 km depth, comprises mainly reworked granulitic and migmatitic Archean basement rocks.

The Wathaman batholith does not have a prominent seismic reflection (Hajnal et al. 1996) or gravity signature, nor is it distinguished in the velocity model (Fig. 7*d*), suggesting that its density and seismic velocity are similar to those of neighbouring domains. However, a coincident weak negative gravity feature, when modelled with a relatively small density contrast (–0.04 g/cm^3), indicates that it could attain a depth of 9 km. Along the geophysical transect, the gravity high that straddles the Wathaman–Rottenstone boundary (see Fig. 3), is modelled as a relatively dense unit within the Rottenstone–La Ronge belt dipping westward beneath the Wathaman (see Fig. 6). These results along with a zone of high resistivity to 5 km depth (Jones et al. 1993) suggest that the Wathaman batholith is <10 km thick. The NFSZ is marginally observed in the seismic reflection image, and a strong contrast in both reflectivity and resistivity are observed in the middle to lower crust directly below the surface trace of the NFSZ.

Western Reindeer Zone

The Glennie domain, Hanson Lake block and the underlying Sask craton, are generally characterized by high resistivity (mainly $>10^3$ Ω.m), low velocities in the lower crust, and upper mantle velocities with >6% azimuthal anisotropy. A prominent conductivity anomaly (North American Central Plains anomaly; 10 Ω.m or less) is situated beneath the Rottenstone – La Ronge domain within the western flank of the crustal culmination observed on the reflection image that defines the Sask craton. This zone is also characterized by low upper crustal velocities. The North American Central Plains conductivity anomaly extends into the zone interpreted as Sask craton, but this may not represent the true spatial extent of the anomaly; it may be a "shadowing" effect caused by the very high conductivity of the anomaly (see Jones et al. (1993) for a higher resolution image). Whereas the westward transition of upper crustal properties from the western Reindeer Zone to the Hearne margin is relatively abrupt, it is poorly defined at lower crustal levels. This is in contrast to the eastern Reindeer Zone, where a clear transition in crustal properties occurs at the Superior margin boundary.

The depth extent of upper crustal moderately resistive zones within the Glennie domain generally corresponds to the depth of the shallowest reflection unit and to an eastward thickening zone of intermediate velocities. However, upper crustal density variations are much thinner. The Hanson Lake block is clearly identified by very high resistivities (10^5 Ω.m), which decrease eastward across the Sturgeon–Weir fault and westward (although less so) across the Tabbernor fault zone. The observed contrast in reflectivity and conductivity that defines the Sturgeon–Weir fault extends to 10–15 km depth. It is not observed in the velocity or density models. The Tabbernor fault zone is clearly imaged by the reflection data and extends to ~30 km depth. It is arguably recognized at shallower crustal levels on the resistivity image.

The reflection Moho beneath the western Reindeer Zone is relatively smooth, and apart from the zone of local crustal thickening, it shows little topography. The refraction Moho is characterized by an abrupt transition from crustal to mantle velocities.

Eastern Reindeer Zone

The Flin Flon domain is characterized by generally moderately resistive (10^5 to $<10^2$ Ω.m), high-velocity crust (Δv of 0.1 to 0.2 km/s), but with relatively large resistivity contrasts occurring within the upper crust. The upper crustal unit immediately east of the Sturgeon–Weir fault is conductive to ~10 km depth, corresponding to the depth of the reflection interpretation. Further east within the Flin Flon domain, a zone of low resistivity (10–100 Ω.m), corresponding to a transparent upper crustal zone on the seismic reflection image continues as far as the Athapapuskow Lake shear zone. These low resistivity–reflectivity rocks correlate with a region of low metamorphic grade volcanic rocks (i.e., upper stratigraphic levels) that have been preserved in a downdropped block within the Flin Flon belt (Lucas et al. 1994).

Further east, a prominent velocity culmination within the Namew gneiss complex correlates partially with an anomalous zone of very low resistivity (the Athapapuskow Lake conductivity anomaly, Ferguson et al. 1999). The upper crustal resistivity pattern within the Namew gneiss complex and the Flin Flon belt does not deepen eastward, as would be suggested by the reflection interpretation, indicating some kind of transition with depth. The small zone of Kisseynew domain rocks at the eastern margin of this zone is conductive (<10 to 10^2 Ω.m), and has intermediate densities (Δρ of 0.04 gm/cm^3) extending to depths consistent with the reflection interpretation, but with no velocity signature. The Superior boundary fault, or the contrast in properties across it, is clearly seen in the conductivity model and reflectivity interpretation, but is only observed to shallow depth in the velocity model. The reflection Moho beneath the eastern Reindeer Zone is relatively complex with significant topography and apparent offsets. In the velocity model, the Moho is characterized by a broad (up to 3 km) transition zone.

Superior margin

The Superior margin is characterized by very high resistivity (mainly $>10^5$ Ω.m) which in conjunction with the reflection images indicate that the Reindeer Zone – Superior margin boundary is a steep east-dipping boundary (White et al. 1999). Elevated upper crustal velocities (Δv of ~0.1 km/s) occur across the Superior boundary zone and extend into the Pikwitonei belt, where increased densities (Δρ of 0.09 gm/cm^3) are observed. Further east, velocities and densities are lower within the lower metamorphic grade Gods Lake domain. Unlike the Hearne margin or Sask craton, no transition to lower resistivities is observed at Moho depths.

Discussion

Comparison of the geophysical models does not radically change our understanding of the geometry of crustal architecture of the THO, but it does serve to provide further confidence in the original interpretation and provide new insights regarding the crustal architecture and the processes responsible for it.

The mean crustal velocity determined for the 800 km transect is 6.5 km/s, which is very close to the mean (6.44 ± 0.24 km/s) for the North American continent (Braile et al. 1989). In contrast, the mean upper mantle velocity at depths of < 50 km is 8.2 km/s which is almost one standard deviation higher than the North American mean of 8.02 ± 0.21 km/s (Braile et al. 1989). Comparing the transect crustal structure to that of *shields and platforms* (40 km-thick crust with a 5–10 km-thick, high-velocity (6.8–7.2 km/s) lower crustal layer; Christensen and Mooney 1995), the THO crust in the west corresponds very closely (mean thickness of ~40 km and a 5–7 km-thick high-velocity basal layer), whereas in the eastern THO, the crust is generally thicker (mean of ~45 km), as is the high-velocity basal layer (>20 km thick). The high-velocity basal layer is completely absent beneath the Sask craton.

There is a notable discrepancy in the depths of the reflection and refraction Mohos (Fig. 7*a*), particularly on the western side of the orogen. The reflection Moho is everywhere deeper than the refraction Moho by 2 to 7 km. Accounting for the uncertainties in the absolute refraction Moho depth and the identification of the reflection Moho, maximum differences of 2–3 km might be expected, where the reflection Moho is well-defined. However, differences exceed this uncertainty by 3–4 km within the western region, where the reflection Moho is clear and where the refraction Moho does not include a transitional zone (in contrast to the east). This implies that either (1) the refraction Moho defined locally by the change in velocity from 7.0–7.2 km/s to 8.2–8.3 km/s and the reflection Moho defined by the abrupt drop-off in reflectivity (i.e., interpreted crustal fabric) locally do not represent the same geological feature, or (2) the crust is characterized by an average velocity anisotropy of ~5% in this region.

Structural implications

Perhaps the most significant results of this study concern the eastern Reindeer Zone. First, the apparent structural complexity of the reflection Moho beneath the Flin Flon belt is real as corroborated by depth information from the refraction velocity model. In the original interpretation of the eastern THO (e.g., White et al. 1994), identification of the reflection Moho was speculative as it was less clear than the relatively flat and prominent Moho in the western THO (e.g., Lucas et al. 1993; Lewry et al. 1994, Hajnal et al. 1996). It was suspected that the Moho in the east occurred below the maximum recording time (16.34 s) used in the 1991 data acquisition. However, with the addition of the refraction velocity model, and a subsequent reflection line acquired along strike to the south (White et al. 2002), it is now clear that the reflection Moho is, in fact, imaged beneath the eastern THO, and it is highly irregular. Unlike the reflection Moho beneath the western THO, which may have acted as a decollement during post-collisional deformation resulting in its flat, prominent appearance (Hajnal et al. 1996), it appears that some of the original Moho topography due to crustal stacking has been preserved beneath the eastern Reindeer zone. This is consistent with the preserved Moho offset along line S3a beneath the northern Kisseynew domain (White et al. 2000*a*). Most of the post-collisional deformation may have been accommodated to the west along the NFSZ and Tabbernor fault zone (i.e., with the exception of the SBF, there are fewer regional-scale orogen-parallel faults in the east).

Secondly, the most prominent upper crustal velocity culmination within the orogen is observed in the vicinity of the Namew gneiss complex (Leclair et al. 1997), where the 6.3 km/s velocity contour breaches the surface rising from a

depth of ~15 km. Interpreting this shallowing of higher velocity rocks as an indication of structural relief, then the Namew gneiss complex represents a shallowing of structural basement by 15 km. Given the east-dipping geometry of crustal panels projecting into this zone (an interpreted crustal-scale stack; Lucas et al. 1993; White et al. 1994), this interpretation suggests east-side up (or east-over-west) displacement along this zone. Previous interpretations have proposed that most of the crustal stacking in this region of the orogen occurred as a result of southwest-vergent thrusting followed by eastward tilting of the stack (Lewry et al. 1994), but the velocity-based interpretation of higher grade rocks in the hanging wall is consistent with east–west crustal stacking. White et al. (2002) argued that east–west stacking (not just late tilting) was significant based on (1) the north–south extent along strike of this east-dipping stack, and (2) the degree of crustal shortening inferred by processes invoked to explain the doubly vergent nature of this margin (Beaumont et al. 1996).

Apart from the Namew gneiss complex, there is little indication of other significant velocity culminations indicative of structural relief across the THO. This is in contrast to the Grenville orogen, for instance, where velocity culminations occur adjacent to major structural boundary zones that have accommodated exhumation of mid-crustal rocks (White et al. 2000*b*). Corrigan and Lucas (1998) have noted the difference in levels of crustal exhumation observed in the Trans-Hudson and Grenville orogens, where regional metamorphic pressures in general are < 600 MPa in the former and commonly > 800 MPa in the latter. They attribute this difference to the longer duration and extent of post-collisional convergence in the Grenville orogen, and the predominance of post-collisional transpression within the THO. Furthermore there is no evidence within the THO for major orogen-normal extensional structures indicative of post-collisional collapse (Hajnal et al. 1996) that might have accommodated major exhumation. All of these observations are generally consistent with the style of crustal deformation (orogen-parallel lateral block extrusion with lower crustal flow) described by Hajnal et al. (1996).

The Sask craton

Comparison of the geophysical models provides further support for the original interpretation of the limited eastward extent of the Sask craton. Given the pronounced changes in conductivity, lower crustal and mantle velocity characteristics east of the Sturgeon–Weir fault, interpretation of an eastward extension of the Sask craton forming basement to the crustal stack is not obvious. If it does continue further east, it is compositionally different. Thus, the provenance of basement rocks that structurally underlie the crustal stack in the eastern THO remains uncertain.

Bezdan and Hajnal (1998) had proposed that a zone of eclogite may exist beneath the interpreted reflection Moho of the Sask craton representing former crust that has been eclogitized. The velocity values for the upper mantle beneath the western orogen (8.1–8.3 km/s) do not preclude this suggestion as the velocities of eclogite and peridotite are similar (mean values from tables 3–5 in Babuska and Cara 1991, are 7.75–8.21 km/s and 8.0–8.28 km/s, respectively). However, the presence of eclogite in the upper mantle beneath the crustal root would increase the density contrast across the Moho as eclogite is generally denser than peridotite (~3.41 g/cm^3 versus ~3.28 g/cm^3 for peridotites; Babuska and Cara 1991). This is inconsistent with the density modelling which required a reduced density contrast across the Moho in this region to match the observed gravity values. Furthermore, this is the region where 6% anisotropy is observed in the upper mantle (Németh et al. 2005), and generally, eclogites are characterized by low anisotropy (2%–4%) compared with peridotites (4%–12%; Babuska and Cara 1991).

Isostatic compensation

The geophysical models clearly show that istostatic compensation associated with the increase in elevation across the orogen does not occur by crustal thickening. In fact, crustal thinning accompanies the regional increase in elevation. Similar conclusions regarding the relationship between elevation and compensation by crustal thickening have been reached in more regional studies elsewhere (e.g., Kane and Godson 1989; Zoback and Mooney 2003). Accepting that the regional isostatic compensation occurs primarily in the mantle, possible causative mechanisms include lateral (1) compositional variations, (2) thermal variations, and (or) (3) topography on mantle density interfaces (e.g., lithosphere–athenosphere boundary). Compositional variation cannot be ruled out, but seems unlikely as there is no obvious way of accounting for a continuous westward change continuing to the eastern Cordillera. Density variations of 0.02–0.005 g/cm^3 for compensation depths below Moho of 50–200 km, respectively, would require a temperature difference of 155–40 °C (using dVp/dT = 0.0005 km/s/°C, which translates to ~0.00013 g/cm^3/°C; Christensen and Mooney 1995). Although not covering the immediate area of our transect, *S*-wave velocity anomaly maps (van der Lee and Nolet 1997) show that the low *S*-wave velocities that characterize the Cordillera in the United States and southern Canada extend as far east as Saskatchewan. Kane and Godson (1989) present the low *S*-wave velocities as evidence for a high-temperature region in the uppermost mantle that accounts for a long-wavelength Bouguer gravity low in the western United States. Thus, a gradual westward increase in mantle temperature by ~40 °C seems a viable explanation.

A change in thickness of the mantle lithosphere is an alternate or complementary explanation for the observed Bouguer gravity low. Using density contrasts of 0.010–0.067 g/cm^3 for the denser mantle lithosphere relative to the less dense asthensophere (Zoback and Mooney 2003 and references therein), then 107 to 16 km, respectively, of westward lithospheric thinning would compensate for the observed surface topography. These values are comparable to an ~50 km westward decrease in the elastic thickness of the lithosphere along the geophysical transect area determined by Pilkington (1991). Thinning of the lithosphere would also result in higher temperatures in the shallow mantle assuming a constant temperature at the base of the lithosphere and constant thermal properties of the lithosphere. Thus, we conclude that the density compensation for the westward increase in elevation is potentially due to a combination of lithospheric thinning and increased upper mantle temperatures.

Conclusions

Comparison of the geophysical data sets and resultant models for the Trans-Hudson Orogen in Manitoba and Saskatchewan results in the following conclusions.

(1) The reflection Moho beneath the eastern THO is highly irregular, and likely preserves Moho topography associated with west-vergent crustal stacking. This contrasts with the western THO, where the Moho appears to have acted as a decollement during post-collisional deformation. West-vergent stacking within the eastern THO is further supported by the presence of higher-grade (higher velocity) rocks (Namew gneiss complex) in the hanging wall of an east-dipping crustal stack. This conclusion is in contrast to previous interpretations (e.g., Lucas et al. 1994; Lewry et al. 1994) for this region. Apart from the Namew gneiss complex, there are no other significant velocity culminations identifying regional structural relief across the THO.

(2) Comparison of the geophysical models supports the original interpretation (e.g., Lucas et al. 1993; Lewry et al. 1994; Hajnal et al. 1996) of the eastward extent of the Sask craton as far as the Sturgeon–Weir fault, east of which a distinct contrast in lower crustal properties occurs.

(3) The regional westward increase in elevation and decrease in Bouguer gravity that occurs across the orogen is associated with decreased crustal thickness, rather than increased crustal thickness that might be predicted by classical isostatic compensation models. The corresponding excess density is compensated within the upper mantle by a westward increase in upper mantle temperatures (by 40–155 °C) and (or) 16–107 km of westward thinning of the mantle lithosphere.

(4) The geological domains of the THO that are exposed on the Canadian Shield can be traced with some confidence southward to at least the 49th parallel. In addition to previously defined domains, a new sub-Phanerozoic domain, the Kindersley domain, lying between the Wollaston and Mudjatik domains is proposed.

Acknowledgments

The authors thank D. Corrigan, A. Hynes, K. Louden, and R. Clowes for providing reviews of an earlier version of this manuscript.

References

Ansdell 2005. Tectonic evolution of the Manitoba–Saskatchewan segment of the Paleoproterozoic Trans-Hudson Orogen, Canada. Canadian Journal of Earth Sciences, **42**: this issue.

Ashton, K.E., Froese, E., and Legault, A. 1999. Recognition of felsic rocks and hydrothermal alteration in moderately to highly metamorphosed parts of the Flin Flon volcanic belt. *In* MinExpo '96 Symposium — Advances in Saskatchewan geology and mineral exploration. *Edited by* K.E. Ashton and C.T. Harper. Saskatchewan Geological Society, Regina, Sask., Special Publication No. 14, pp. 27–43.

Babuska, V., and Cara, M. 1991. Seismic Anisotropy in the Earth. Kluwer Academic Publishers, Dordrecht.

Barton, P.J. 1986. The relationship between seismic velocity and density in the continental crust — a useful constraint? Geophysical Journal of the Royal Astronomical Society, **87**: 195–208.

Beaumont, C., Ellis, S., Hamilton, J., and Fullsack, P. 1996. Mechanical model for subduction-collision tectonics of Alpine-type compressional orogens. Geology, **24**: 675–678.

Bezdan, S., and Hajnal, Z. 1998. Expanding spread profiles across the Trans-Hudson Orogen. Tectonophysics, **288**: 83–91.

Bleeker, W. 1990. New structural-metamorphic constraints on Early Proterozoic oblique collision along the Thompson Nickel belt, Manitoba, Canada. *In* The Early Proterozoic Trans-Hudson Orogen of North America. *Edited by* J.F. Lewry and M.R. Stauffer. Geological Association of Canada, Special Paper 37, pp. 57–73.

Braile, L.W., Hinze, W.J., von Frese, R.R.B., and Keller, G.R. 1989. Seismic properties of the crust and uppermost mantle of the conterminous United States and adjacent Canada. *In* Geophysical framework of the continental United States. *Edited by* L.C. Pakiser and W.D. Mooney. The Geological Society of America, Boulder, Colo., Memoir 172, pp. 655–680.

Christensen, N.I. 1966. Elasticity of ultrabasic rocks. Journal of Geophysical Research, **71**: 5921–5931.

Christensen, N.I., and Fountain, D.M. 1975. Constitution of the lower continental crust based on experimental studies of seismic velocities in granulite. Bulletin of the Geological Society of America, **86**: 227–236.

Christensen, N.I., and Mooney, W.D. 1995. Seismic velocity structure and composition of the continental crust: a global view. Journal of Geophysical Research, **100**: 9761–9788.

Cook, F.A., Varsek, J.L., Clowes, R.M., Kanasewich, E.R., Spencer, C.S., Parrish, R.R., Brown, R.L., Carr, S.D., Johnson, B.J., and Price, R.A. 1992. Lithoprobe crustal reflection cross section of the southern Canadian Cordillera, 1, Foreland thrust and fold belt to Fraser River fault. Tectonics, **11**: 12–35.

Corkery. M.T. 1987. Geological Highway map of Manitoba. Geological Survey of Canada – Manitoba Minerals Division, Mineral Development Agreement, Special Publication No. 1, map scale 1 : 1 000 000.

Corrigan, D., and Lucas, S.B. 1998. Contrasting styles of continent-continent collision: the Trans-Hudson and Grenville orogens. Geological Association of Canada – Mineralogical Association of Canada, 1998 Joint Annual Meeting, Quebec City, Que., 18–20 May 1998 Abstract Vol., pp. A37–A38.

Coté, M.L. 1994. Kinematics and shear-induced structures of the Birch Rapids straight belt, north-central Saskatchewan. *In* Lithoprobe Trans-Hudson Orogen Transect, Report of 4th Transect Meeting, April 11–12, 1994, Saskatoon, Sask. *Edited by* Z. Hajnal and J. Lewry. Lithoprobe Secretariat for the Canadian Lithoprobe Program, The University of British Columbia, Vancouver, B.C., Lithoprobe report No. 38, pp. 161–170.

Eaton, D.W., and Hynes, A. 2000. The 3-D crustal structure in the Manicouagan region: new seismic and gravity constraints. Canadian Journal of Earth Sciences, **37**: 307–324.

Ferguson, I.J., Jones, A.G., Sheng, Y., Wu, X., and Shiozali, I. 1999. Geoelectric response and crustal electrical-conductivity structure of the Flin Flon belt, Trans-Hudson Orogen, Canada. Canadian Journal of Earth Sciences, **36**: 1917–1938.

Gazdag, J. 1978. Wave equation migration with the phase-shift method. Geophysics, **43**: 1342–1351.

Hajnal, Z., Lucas, S.B., White, D.J., Lewry, J., Bezdan, S., Stauffer, M.R., and Thomas, M.D. 1996. Seismic reflection images of strike-slip faults and linked detachments in the Trans-Hudson Orogen. Tectonophysics, **15**: 427–439.

Hajnal, Z., J. Lewry, White, D.J., Ashton, K., Clowes, R., Stauffer, M., Gyorfi, I., and Takacs, E. 2005. The Sask craton and Hearne Province margin: seismic reflection studies in the western

Trans-Hudson Orogen. Canadian Journal of Earth Sciences, **42**: this issue.

Hoffman, P.F. 1988. United Plates of America, the birth of a craton: Early Proterozoic assembly and growth of Laurentia. Annual Reviews of Earth and Planetary Sciences, **16**: 543–603.

Jones, A.G., Craven, J.A., McNeice, G.A., Ferguson, I.J., Boyce, T., Farquharson, C., and Ellis, R.G. 1993. The North American Central Plains conductivity anomaly within the Trans-Hudson orogen in northern Saskatchewan. Geology, **21**: 1027–1030.

Jones, A.G., Ledo, J., and Ferguson, I.J. 2005. Electromagnetic images of the Trans-Hudson Orogen: The North American Central Plains (NACP) anomaly revealed. Canadian Journal of Earth Sciences, 42: this issue.

Kane, M.F., and Godson, R.H. 1989. A crust/mantle structural framework of the conterminous United States based on gravity and magnetic trends. *In* Geophysical framework of the continental United States. *Edited by* L.C. Pakiser and W.D. Mooney. The Geological Society of America, Boulder, Colo., Memoir 172, pp. 383–403.

Kreis, L.K., Ashton, K.E., and Maxeiner, R.O. 2000. Geology of the Precambrian basement and Phanerozoic strata in Saskatchewan. Lower Paleozoic Map Series, Saskatchewan Energy and Mines, Open File Report 2000-2, sheet 1 of 8.

Leclair, A.D., Lucas, S.B., Broome, H.J., Viljoen, D.W., and Weber. W. 1997. Regional mapping of Precambrian basement beneath Phanerozoic cover in southeastern Trans-Hudson Orogen, Manitoba and Saskatchewan. Canadian Journal of Earth Sciences, **34**: 618–634.

Lemieux, S., Ross, G.M., and Cook, F.A. 2000. Crustal geometry and tectonic evolution of the Archean crystalline basement beneath the southern Alberta Plains, from new seismic reflection and potential-field studies. Canadian Journal of Earth Sciences, **37**: 1473–1491.

Lewry, J.F., Hajnal, Z., Green, A., Lucas, S.B., White, D., Stauffer, M.R., Ashton, K.E., Weber, W., and Clowes, R. 1994. Structure of a Paleoproterozoic continent-continent collision zone: a LITHOPROBE seismic reflection profile across the Trans-Hudson Orogen, Canada. Tectonophysics, **232**: 143–160.

Louden, K.E., and Fan, J. 1998. Crustal structures of Grenville, Makkovik, and southern Nain provinces along the Lithoprobe ECSOOT Transect: regional seismic refraction and gravity models and their tectonic implications. Canadian Journal of Earth Sciences, **35**: 583–601.

Lucas, S.B., Green, A., Hajnal, Z., White, D.J., Lewry, J., Ashton, K., Weber, W., and Clowes, R. 1993. Deep seismic profile across a Proterozoic collision zone: surprises at depth. Nature, **363**: 339–342.

Lucas, S.B., White, D., Hajnal, A., Lewry, J., Green, A., Zwanzig, H., Ashton, K., Schledewitz, D., Norman, A., Williams, P., Clowes, R., Stauffer, M., and Spence, G. 1994. Three-dimensional structure of the Trans-Hudson orogen: implications for collisional and post-collisional deformation history. Tectonophysics, **232**: 161–178.

Lucas, S.B., Syme, E.C., and Ashton, K.E. 1999. New perspectives on the Flin Flon Belt, Trans-Hudson Orogen, Manitoba and Saskatchewan: an introduction to the special issue on the NATMAP Shield Margin Project, Part 1. Canadian Journal of Earth Sciences, **36**: 135–140.

Ludwig, W.J., Nafe, J.E., and Drake, C.L. 1970. Seismic refraction. *In* The Sea. Vol. 4, New concepts of sea floor evolution. *Edited by* A.E. Maxwell. Wiley-Interscience, New York, Part 1, pp. 53–84.

Macdonald, R., and Broughton, P. 1980. Geological map of Saskatchewan. Provisional edition. Saskatchewan Minerals and Resources, map scale 1 : 1 000 000.

McGrath, P.H. 1991. Dip and depth extent of density boundaries using horizontal derivatives of upward-continued gravity data. Geophysics, **56**: 1533–1542.

Miles, W, Stone, P.E., and Thomas, M.D. 1997. Magnetic and gravity maps with interpreted Precambrian basement, Saskatchewan (5 sheets, map scale 1 : 1 500 000). Geological Survey of Canada, Open File 3488.

Németh, B. 1999. Structure of the lithosphere within the Trans-Hudson Orogen (Results of the 1993 Lithoprobe Trans-Hudson refraction experiment). Ph.D. thesis, University of Saskatchewan, Sask.

Németh, B., Clowes, R.M., Hajnal, Z. 2005. Lithospheric structure of the Trans-Hudson Orogen from seismic refraction – wide angle reflection studies. Canadian Journal of Earth Sciences, **42**: this issue.

Pilkington, M. 1991. Mapping elastic lithospheric thickness variations in Canada. Tectonophysics, **190**: 283–297.

Pilkington, M., and Thomas, M.D. 2001. Magnetic and gravity maps with interpreted Precambrian basement, Manitoba. Geological Survey of Canada, Open File Report 3739.

Rodi, W., and Mackie, R.L. 2001. Nonlinear conjugate gradients algorithm for 2-D magnetotelluric inversion. Geophysics, **66**: 174–187.

Ross, G.M., Milkereit, B., Eaton, D., White, D., Kanasewich, E.R., and Burianyk, M.J.A. 1995. Paleoproterozoic collisional orogen beneath the western Canada sedimentary basin imaged by Lithoprobe crustal seismic-reflection data. Geology, **23**: 195–199.

Simpson, R.W., Jachens, R.C., Blakely, R.J., and Saltus, R.W. 1986. A new isostatic residual gravity map of the conterminous United States with a discussion on the significance of isostatic residual anomalies. Journal of Geophysical Research, **9**: 8348–8372.

Surasky, A.T., Hosain, I.T., and Letkemen, A.J. 2001. Gravity and magnetic profile along The Pas moraine. *In* Report of activities 2001. Manitoba Industry, Trade and Mines, Manitoba Geological Survey, pp. 164–171.

Thomas, M.D., and Tanczyk, E.I. 1994. Progress in gravity and magnetic analysis along the Lithoprobe Trans-Hudson orogen transect. *In* Lithoprobe Trans-Hudson Orogen Transect. Report of 4th Transect Meeting, April 11–12, 1994, Saskatoon, Sask. *Edited by* Z. Hajnal and J. Lewry. Lithoprobe Secretariat for the Canadian Lithoprobe Program, The University of British Columbia, Vancouver, B.C., Lithoprobe report No. 38, pp. 135–150.

Thomas, M.D. 2001. Potential field images of the Proterozoic Trans-Hudson orogen. *In* Canadian Shield: significance for mapping buried extensions and plate tectonic models. American Geophysical Union Spring Meeting, Boston, Mass., May 29th – June 2nd, 2001.

van der Lee, S., and Nolet, G. 1997. Upper mantle *S* velocity of North America, Journal of Geophysical Research, **102**: 22815–22838.

White, D.J., Lucas, S.B., Hajnal, Z., Green, A.G., Lewry, J.F., Weber, W., Zwanzig, H.V., Bailes, A.H., Syme, E.C., Macek, J., Ashton, K.E., and Thomas, D.J. 1994. Early Proterozoic thick-skinned tectonics: LITHOPROBE seismic reflection results from the eastern Trans-Hudson Orogen. Canadian Journal of Earth Sciences, **31**: 458–469.

White, D.J., Jones, A.G., Lucas, S.B., and Hajnal, Z. 1999. Tectonic evolution of the Superior Boundary zone from coincident seismic reflection and magnetotelluric profiles. Tectonics, **18**: 430–451.

White, D.J., Zwanzig, H., and Hajnal, Z. 2000*a*. Seismic images of

a Paleoproterozoic suture zone: the Kisseynew Domain northern boundary, Trans-Hudson Orogen, Geology, **28**: 527–530.

White, D.J., Forsyth, D.A., Asudeh, I., Carr, S.D., Wu, H., Easton, R.M., and Mereu, R.F. 2000*b*. A seismic-based cross-section of the Grenville Orogen in southern Ontario and western Quebec. Canadian Journal of Earth Sciences, **37**: 183–192.

White, D.J., Lucas, S.B., Bleeker, W., Hajnal, Z., Lewry, J.F., and Zwanzig, H.V. 2002. Suture-zone geometry along an irregular Paleoproterozoic margin: The Superior boundary zone, Manitoba, Canada. Geology, **30**: 735–738.

Zelt, C.A., and White, D.J. 1995. Crustal structure and tectonics of the southeastern Canadian Cordillera, Journal of Geophysical Research, **100**: 24255–24273.

Zoback, M.L., and Mooney, W.D. 2003. Lithospheric buoyancy and continental intraplate stresses. International Geology Review, **45**: 95–118.